

**STRONGLY CORRELATED SYSTEMS AND HIGH TEMPERATURE SUPERCONDUCTIVITY****Features of the magnetic properties of rare-earth intermetallides  $\text{RMn}_2\text{Ge}_2$  (Review)**

N. P. Kolmakova and A. A. Sidorenko

*Bryansk State Engineering University, 241035 Bryansk, Russia*

R. Z. Levitin\*

*Physics Department, M. V. Lomonosov Moscow State University, Vorob'evy Gory, 119899 Moscow, Russia*

(Submitted December 24, 2001; revised February 24, 2002)

*Fiz. Nizk. Temp.* **28**, 905–925 (August–September 2002)

The magnetic and other physical properties of the ternary intermetallic compounds  $\text{RMn}_2\text{Ge}_2$  (R is a rare earth) are of great interest on account of effects due to the coexistence of the  $3d$  (manganese) and  $4f$  (rare-earth) magnetic subsystems. The layered structure, the high sensitivity of the exchange parameters to the interatomic distances, the antiferromagnetic exchange interaction in the manganese subsystem in intermetallides containing heavy rare earths, and also the appreciable crystal-field effects in the rare-earth subsystem make for complex magnetic phase diagrams in these compounds. A review is given of the experimental and theoretical research on the magnetic properties and magnetic phase diagrams of the intermetallic compounds  $\text{RMn}_2\text{Ge}_2$ , including measurements in high and ultrahigh magnetic fields. A theoretical model is proposed which takes into account the features of the crystal structure and the hierarchy of exchange interactions in intermetallides containing heavy rare earths; this model is in many cases capable of describing the magnetic properties of these intermetallides over a wide range of magnetic fields and temperatures, and it permits determination of the interaction parameters for  $\text{RMn}_2\text{Ge}_2$  compounds with  $\text{R}=\text{Gd}$  and  $\text{Dy}$  from a comparison of the experimental and calculated magnetization curves and  $H$ – $T$  phase diagrams. © 2002 *American Institute of Physics*. [DOI: 10.1063/1.1511711]

**1. INTRODUCTION**

Ternary intermetallic compounds containing rare earths (R) and transition elements (T) have attracted a great deal of interest in recent years. This is because the inclusion of a third element (X) in the formula for the intermetallide allows one to vary the type of crystal structure, interatomic distances, concentration of conduction electrons, etc., making it possible to obtain materials with new magnetic properties.

Among the many ternary intermetallides the compounds  $\text{RT}_2\text{X}_2$  with  $\text{X}=\text{Ge}$  or  $\text{Si}$  have held a steady research interest, as can be seen from the number of scientific publications devoted to them in recent years (see, e.g., the review<sup>1</sup>). This attention is due to the fact that the intermetallides  $\text{RT}_2\text{X}_2$  manifest a great diversity of physical characteristics. Among these compounds one can find superconductors and heavy-fermion systems, variable-valence effects, etc.<sup>1</sup> The magnetic properties of these intermetallides are also extremely interesting, although one cannot yet say that the magnetism of the intermetallic compounds  $\text{RT}_2\text{X}_2$  is conclusively understood.

The magnetic properties of  $\text{RT}_2\text{X}_2$  intermetallides containing manganese are especially interesting, since only in  $\text{RMn}_2\text{X}_2$  does magnetic ordering arise in the  $3d$  manganese subsystem at comparatively high temperatures.<sup>1</sup> The features of the crystal structure and exchange interactions of  $\text{RMn}_2\text{X}_2$  are conducive to spontaneous magnetic phase transitions in many of these compounds, and several of those transitions have not yet been adequately explained. The magnetic phase

transitions in a magnetic field have been studied even less. The magnetoelastic properties of  $\text{RMn}_2\text{X}_2$  intermetallides have also been studied in insufficient detail. Very recently it was pointed out that because of the features of the crystal structure, these intermetallides are natural superlattices and can be used as model objects for studying the processes occurring in superlattices; this circumstance has heightened the interest in these objects.

The intermetallic compounds  $\text{RMn}_2\text{X}_2$  that have been studied in greatest detail are those with  $\text{X}=\text{Ge}$ . In this article we give a brief review of the nature and the features of the magnetic ordering in intermetallides of the  $\text{RMn}_2\text{Ge}_2$  type, based on both information available in the literature and the experimental and theoretical research of the authors. A theoretical model is proposed which in many cases is capable of describing the spontaneous and induced magnetic phase transitions in these compounds.

**2. CRYSTAL STRUCTURE OF THE INTERMETALLIC COMPOUNDS  $\text{RT}_2\text{X}_2$** 

Intermetallic compounds of the type  $\text{RT}_2\text{X}_2$  are formed by the rare earths (R) thorium, uranium, yttrium, barium, and calcium, transition elements (T) of the  $3d$ ,  $4d$ , and  $5d$  groups, and germanium or silicon (X). These intermetallides containing manganese and other  $3d$  materials crystallize in the well-known body-centered tetragonal structure that was

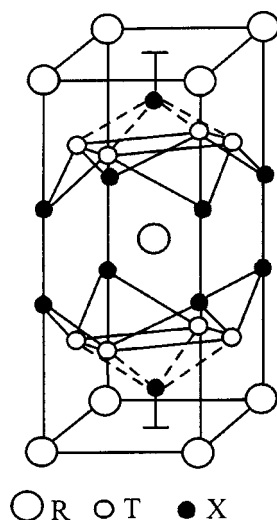


FIG. 1. Crystal structure of the  $\text{ThCr}_2\text{Si}_2$  type.

first determined for  $\text{ThCr}_2\text{Si}_2$  in Ref. 2 and have space group  $I4/mmm$ . The unit cell of this structure contains two formula units and is illustrated in Fig. 1.

An important feature of the compounds  $\text{RMn}_2\text{X}_2$  with a structure of the  $\text{ThCr}_2\text{Si}_2$  type is that this structure consists of layers of rare earths, transition elements, and germanium (or silicon) lying perpendicular to the tetragonal axis  $c$  and arranged in the sequence



The layers of X and T atoms form a sandwich structure with a rare-earth atom situated between neighboring sandwiches. Each R atom is surrounded by eight X atoms and eight T atoms, which are located at the corners of a cube. The interatomic distances R–X and R–T are smaller than the sum of the corresponding ionic radii but larger than the sum of the covalent radii.

### 3. MAGNETIC PROPERTIES AND MAGNETIC STRUCTURE OF THE INTERMETALLIC COMPOUNDS $\text{RMn}_2\text{Ge}_2$

As we said in the Introduction, numerous studies have shown that in the majority of the  $\text{RT}_2\text{Ge}_2$  intermetallic compounds the transition metal T does not have a magnetic moment. An exception is manganese, which is magnetically ordered at relatively high temperatures.<sup>1</sup> Thus from a magnetic standpoint the  $\text{RMn}_2\text{Ge}_2$  intermetallics consist of two different subsystems: the R subsystem and the Mn subsystem. A feature of the magnetic properties of the  $\text{RMn}_2\text{Ge}_2$  intermetallics is that these subsystems become magnetically ordered at different temperatures: at high temperatures only the manganese subsystem is ordered; the ordering of the rare-earth subsystem occurs at much lower temperatures. The main magnetic characteristics of the  $\text{RMn}_2\text{Ge}_2$  intermetallics, according to the data of different experiments, are presented in Table I.

Neutron diffraction and magnetic studies of  $\text{RMn}_2\text{Ge}_2$  compounds with light rare earths<sup>9,10</sup> have shown that with decreasing temperature in those compounds the manganese subsystem undergoes first a transition from the paramagnetic to an antiferromagnetic state (the Néel temperature  $T_N$ ) and

then, as the temperature is decreased further, a transition to a ferromagnetic state (the Curie temperature  $T_C$ ). The Néel temperature of these compounds lies in the range 390–410 K, and  $T_C \approx 330$  K.

The magnetic ordering of the rare-earth subsystem in  $\text{RMn}_2\text{Ge}_2$  compounds with the light rare earths Pr and Nd occurs at a temperature  $T_i$  of the order of 100 K.<sup>10</sup> The compound  $\text{SmMn}_2\text{Ge}_2$  has the most complex magnetic behavior.<sup>13,15</sup> Like the other intermetallics with light rare earths, this compound undergoes a transition from the paramagnetic to an antiferromagnetic state and then from the antiferromagnetic to a ferromagnetic state as the temperature is lowered. However, unlike the intermetallics with La, Pr, and Nd, when  $\text{SmMn}_2\text{Ge}_2$  is cooled below a temperature  $T_{i1} \approx 150$  K the manganese subsystem undergoes a transition from a ferromagnetic to an antiferromagnetic state (meanwhile, the Sm subsystem is magnetically disordered). When the temperature is decreased further to  $T_i \approx 100$  K an inverse transition of the Mn subsystem to a ferromagnetic state occurs, accompanied by ferromagnetic ordering of the Sm subsystem, so that a resultant ferromagnetic structure is formed.

The  $\text{RMn}_2\text{Ge}_2$  intermetallics with heavy rare earths are simpler from a magnetic point of view. On cooling to the Néel temperature  $T_N$ , antiferromagnetic ordering arises in their Mn subsystem.<sup>1</sup> The value of  $T_N$  is equal to 410 K for the Tb compound and increases with increasing atomic number of the rare earth, to  $T_N \approx 478$  K for  $\text{TmMn}_2\text{Ge}_2$  (Refs. 19 and 21). The compound  $\text{GdMn}_2\text{Ge}_2$  stands out some, with  $T_N \approx 365$  K.<sup>5,18</sup> However, an anomaly of the magnetization of this intermetallic has been detected<sup>17</sup> at a temperature  $T_N \approx 480$ –500 K. The nature of this anomaly is not clear.

On further cooling of  $\text{RMn}_2\text{Ge}_2$  intermetallics with heavy rare earths to  $T_i$ , magnetic ordering occurs in the rare-earth subsystem.<sup>19,21</sup> This temperature is approximately equal to 95 K for the Gd and Tb compounds, around 40 K for  $\text{DyMn}_2\text{Ge}_2$ , and considerably lower for compounds with Ho ( $T_i = 2.15$  K), Er ( $T_i = 5.5$  K), and Tm ( $T_i = 8.5$  K).<sup>21</sup> We note that in the compounds containing Gd, Tb, and Dy the onset of magnetic order in the R subsystem is a first-order phase transition and is accompanied by a transition of the Mn subsystem from the antiferromagnetic to the ferromagnetic state, so that the resulting magnetic structure becomes ferrimagnetic. In the remaining compounds with heavy rare earths the magnetic ordering of the rare-earth subsystem is a second-order phase transition; here the Mn subsystem remains antiferromagnetic to the lowest temperatures investigated ( $\sim 2$  K).<sup>21</sup>

Previously it has been assumed that the magnetic structure of the Mn subsystem consists of ferromagnetically ordered manganese planes of the (001) type, and the resulting ferro- or antiferromagnetic structure is realized for a parallel or antiparallel orientation of the magnetic moments of neighboring planes, respectively. However, recent neutron diffraction studies<sup>8–10</sup> have shown that the situation is more complicated. From neutron diffraction measurements both on pure  $\text{RMn}_2\text{Ge}_2$  compounds and on mixed compounds of the  $(\text{Y, La})\text{Mn}_2\text{Ge}_2$  and  $(\text{R, R}')\text{Mn}_2\text{Ge}_2$  type it follows that collinear magnetic ordering of the Mn subsystem occurs only in compounds with the heavy rare earths Tb, Dy, Ho, Er, Tm, and Y (the intermetallic  $\text{GdMn}_2\text{Ge}_2$  was not studied by neu-

TABLE I. Main magnetic characteristics of the compounds  $\text{RMn}_2\text{Ge}_2$ :  $T_N$  is the Néel temperature,  $T_C$  the Curie temperature,  $T_I$  the temperature of ordering of the R subsystem,  $\Theta_p$  the paramagnetic Curie temperature,  $M_{\text{eff}}$  the effective moment,  $M_s$  the spontaneous magnetization at 4.2 K,  $m_{\text{Mn}}$  and  $m_{\text{R}}$  the magnetic moments of the Mn and R atoms at 4.2 K,  $g_J J$  the magnetic moment of  $\text{R}^{3+}$ , and EA the axis of easy magnetization.

R	$T_N$ , K	$T_C$ , K	$T_I$ , K	$\Theta_p$ , K	$M_{\text{eff}}$ , $\mu_B$	$M_s$ , $\mu_B$	$m_{\text{Mn}}$ , $\mu_B$	$m_{\text{R}}$ , $\mu_B$	$g_J J$ , $\mu_B$	EA	
La	413 [3]	310 [5,6]		270 [6]	3,5 [6]	3,1 [6]	3,065 [9]			[001]	
	410 [4]	306 [7]		225 [9]	4,7 [7]	3,0 [5,7]	1,55 [6]				
		326 [8]			3,39 [9]						
Pr	414 [3]	330 [10]	100 [10]	260 [10]	6,1 [10]	5,9 [11]	2,80 [10]	2,95 [10]	3,2	[001]	
	415 [4]	329 [11]	80 [11]			3,7 [10]	1,55 [11]	2,77 [11]			
		334 [5]	40 [5]			3,9 [5]					
Nd	418 [3]	330 [10]	100 [10]	280 [10]	6,0 [10]	5,7 [12]	2,70 [10]	2,35 [10]	3,28	[001], $\perp c^{**}$	
	415 [4]	336 [12]	40 [5]			5,2 [10]	1,55 [3]				
		334 [5]				6,0 [5]					
Sm	389 [3]	348 [13]	60; 196* [13]		3,4 [7]	3,0 [7]	1,7 [13]		0,71	[001], [110]***	
	385 [4]	350 [14]	100; 153 [14]								
		341 [15]	100; 153 [15]								
Gd	365 [5,16]		95	100 [19]	8,8 [19]	3,6 [19]	2,0 [18]	7,0 [17]	7	[001]	
			[5,16,17,18]								1,7 [17]
Tb	414 [19]		95 [19]	100 [19]	10,4 [19]	5,3 [19]	2,21 [21]	8,81 [21]	9	[001]	
	413 [20]		110 [20]		9,6 [7]	6,0 [7]	2,3 [20]	8,0 [19]			
			105 [21]			1,7 [19]	7,8 [20]				
Dy	438 [19,22]		40 [19]	100 [19]	10,8 [19]		2,2 [24]	10,2 [18,24]	10	[001]	
	430 [23,24]		47 [5,7]		9,9 [5,7]	6,2 [19]	2,0 [22]	3,5 [5,7]			
	385 [5,7]										
Ho	459 [19]		4,2 [19]	100 [19]	10,0 [19]				10	[001]	
	403 [5,7]		2,1 [21]		8,5 [5,7]	5,5 [5,7]	2,38 [21]	6,9 [21]			
			37 [5,7]								
Er	475 [19]		5,5 [21]	224 [19]	9,4 [19]	8,3 [19]	2,3 [7]	6,81 [21]	9	$\perp c$	
	390 [7]		8,5 [7]		9,0 [7]	6,0 [7]	2,34 [21]	7,7 [7]			
			4,2 [19]								
Tm	487 [21]		8,5 [21]		6,2 [7]		2,28 [21]	6,63 [21]	7	[001]	
	458 [7]										
Y	427 [3]			394 [3]	3,34 [3]		2,23 [21]				
	437 [25]			385 [7]	3,8 [7]	0,11 [25]	2,95 [7]				
	395 [7]										

Notes: \*In  $\text{SmMn}_2\text{Ge}_2$  on cooling to this temperature a transition occurs from the ferromagnetic phase to an antiferromagnetic phase in the manganese subsystem; \*\*below 250 K; \*\*\*below 100 K.

tron diffraction because of the large neutron absorption cross section of gadolinium). At the same time, in intermetallides with light rare earths more complex magnetic structures are formed in the manganese subsystem. These magnetic structures have the feature that in many of the compounds a magnetic ordering which combines ferro- and antiferromagnetic components arises in planes of the (001) type; in addition, in some of the compounds there can be long-period noncollinear structures. Figure 2 shows the different types of magnetic structures of the Mn subsystem which are characteristic of the (Y, La) $\text{Mn}_2\text{Ge}_2$  system and of other  $\text{RMn}_2\text{Ge}_2$

intermetallides.<sup>8,10,26</sup> In the compound  $\text{YMn}_2\text{Ge}_2$  there is a collinear antiferromagnetic structure of the AFil type. This is the type of structure that the Mn subsystem has in intermetallides containing heavy rare earths at temperatures above  $T_I$ . Below  $T_I$  the Mn subsystem in compounds containing Tb, Dy, and, apparently, Gd undergoes a transition to a collinear ferromagnetic structure of the F type.<sup>21</sup> The AFil-type antiferromagnetic structure of the Mn subsystem in compounds containing Ho, Er, and Tm persists to the lowest temperatures ( $\sim 2.2$  K). In the compound  $\text{LaMn}_2\text{Ge}_2$  at high

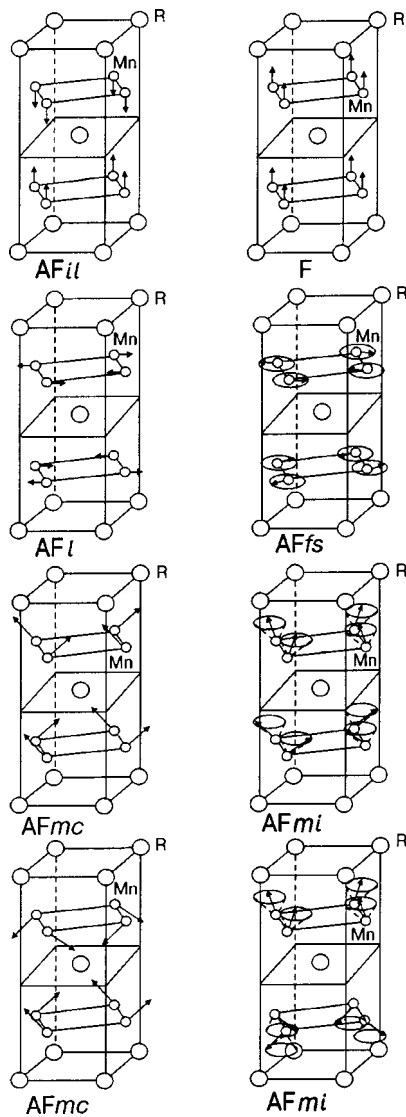


FIG. 2. Magnetic structures of the manganese subsystem observed in  $\text{RMn}_2\text{Ge}_2$  intermetallic compounds.

temperatures ( $T_N > T > T_C$ ) there is a planar spiral antiferromagnetic structure of the *AFfs* type, which at a temperature below  $T_C$  undergoes a transition to an incommensurate structure of the *Fmi* type with a ferromagnetic component along the tetragonal axis. In the compounds  $\text{PrMn}_2\text{Ge}_2$  and  $\text{NdMn}_2\text{Ge}_2$  for temperatures above  $T_C$  the Mn subsystem has a collinear antiferromagnetic structure of the *AFf* type in which the magnetic moment is perpendicular to the  $c$  axis. Below  $T_C$  these compounds have a commensurate ferromagnetic structure of the *Fmc* type, with a ferromagnetic component along the  $c$  axis. At still lower temperatures ( $T < 280$  and  $250$  K for Pr and Nd, respectively) a helical ferromagnetic structure of the *Fmi* type arises in the Mn subsystem.

The magnetic ordering in the rare earth subsystem is also differential in different compounds. In intermetallics containing Pr, Nd, Gd, Tb, Dy, and Er at a temperature below  $T_f$  the R subsystem has a collinear ferromagnetic structure. The magnetic moments of Nd and Er lie in the (001) plane, and in the rest of these compounds the magnetic moment of the rare earth is oriented along the tetragonal axis.<sup>10,21</sup> In  $\text{HoMn}_2\text{Ge}_2$

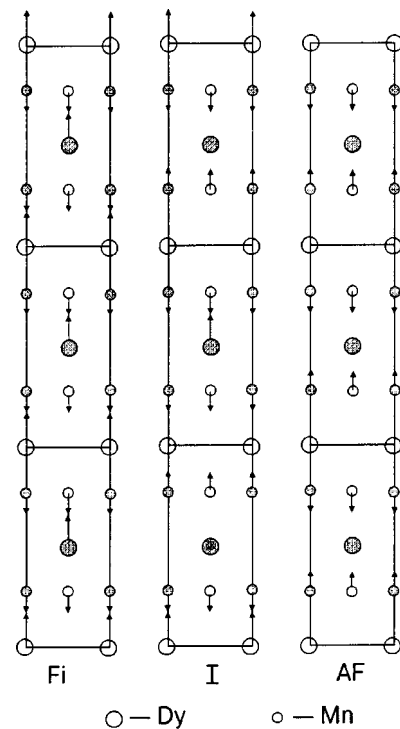


FIG. 3. Magnetic structures of the compound  $\text{DyMn}_2\text{Ge}_2$  (the shaded atoms are shifted relative to the plane of the figure by half a lattice parameter).

below  $T_f$  there are two different coexisting sinusoidally modulated magnetic structures in the Ho subsystem.<sup>21</sup> In  $\text{TmMn}_2\text{Ge}_2$  the Tm moments lie in the basal plane.<sup>21</sup> Along the  $c$  axis the ferromagnetic Tm (001) layers alternate in the sequence  $++--$ . The Mn moments deviate slightly from the  $c$  axis, and the components of the Mn moments in the (001) layer alternate from layer to layer in the same sequence as for the moments of Tm.

It has also been found as a result of magnetic and neutron diffraction studies<sup>22,24</sup> that the magnetic structure in  $\text{DyMn}_2\text{Ge}_2$  at  $T < T_1 = 33\text{--}35$  K is ferrimagnetic: the magnetic moments of the manganese and dysprosium subsystems are collinear to the tetragonal axis and antiparallel to each other (Fig. 3, the Fi phase). Above  $T_2 = 37.5\text{--}40$  K the manganese subsystem is antiferromagnetic, and the dysprosium subsystem is in a paramagnetic state (Fig. 3, the AF phase). According to the data of Ref. 22, for  $T_1 < T < T_2$  the ferrimagnetic and antiferromagnetic phases coexist with a phase in which the magnetic moments of the manganese subsystem alternate in the sequence  $--+--+$ , and the dysprosium subsystem is partially ordered: 1/3 of the dysprosium atoms are magnetically ordered, and 2/3 are found in a paramagnetic state (Fig. 3, phase I).

The compound  $\text{SmMn}_2\text{Ge}_2$  has not been studied by neutron diffraction. However, studies of the mixed silicon-based compound  $\text{Nd}_{0.35}\text{La}_{0.65}\text{Mn}_2\text{Si}_2$  (Ref. 26), in which temperature-induced spontaneous magnetic phase transitions like those in  $\text{SmMn}_2\text{Ge}_2$  were observed, have shown that in this compound the Mn system has different magnetic structures at different temperatures, much as has been observed in germanium-based intermetallics with light rare earths (see Fig. 2). Below  $T_N \approx 395$  K the compound  $\text{Nd}_{0.35}\text{La}_{0.65}\text{Mn}_2\text{Si}_2$  is characterized by the structure *AFf*, in

the temperature interval between  $T_C \approx 295$  K and  $T_{t1} \approx 220$  K by the structure  $Fmc$ , for  $T_{t1} > T > T_{t2} \approx 50$  K it has the  $AFmc$  structure, and for  $T < T_{t2}$  it again has the  $Fmc$  structure (the magnetic structures mentioned are illustrated in Fig. 2). It is possible that the Mn subsystem in  $\text{SmMn}_2\text{Ge}_2$  has these same structures.

In intermetallides with light rare earths the R–Mn exchange interaction is ferromagnetic, and as a consequence of this the resulting magnetic structure below the magnetic ordering temperature of the rare-earth subsystem is ferromagnetic. In intermetallides with heavy rare earths, on the contrary, the R–Mn exchange interaction is antiferromagnetic, so that the resulting magnetic structure is ferrimagnetic.

Neutron diffraction studies<sup>8,10</sup> have determined the magnetic moments of Mn at  $T=4.2$  K in the compounds  $\text{LaMn}_2\text{Ge}_2$ ,  $\text{PrMn}_2\text{Ge}_2$ , and  $\text{NdMn}_2\text{Ge}_2$ , which have the values 3.06, 2.8, and  $2.7\mu_B$ , respectively, which are much larger than the values obtained from the magnetic measurements. This difference can be explained by the circumstance that in the compounds studied the Mn subsystem has a non-collinear structure, as the neutron diffraction studies have revealed.

In compounds with heavy rare earths the magnetic moment of manganese is approximately  $1.7-2\mu_B$ , according to magnetic measurements on single crystals.<sup>19,27</sup> At the same time, from the neutron diffraction data the moment of the manganese is almost the same in all these compounds, having a value  $2.3\mu_B$ .<sup>21</sup> We note that according to the neutron diffraction data the magnetic moment of manganese in compounds with light rare earths is much larger than the moment of manganese in the compounds with heavy rare earths. A possible explanation of this is that the manganese is found in different electronic states in the compounds with light and heavy rare earths. This effect may be due to the change in the distance between manganese atoms as one goes from La to Tm. We see from Table I that the magnetic moments of the rare earths are close to the theoretical values  $g_J\mu_B$  for the free  $\text{Re}^{3+}$  ions (except Nd and Ho). Some differences may be attributed to the influence of the crystalline field on the state of the  $\text{R}^{3+}$  ions. In Ref. 28 it was observed that the magnetic moment of manganese ( $\Delta m_{\text{Mn}}/m_{\text{Mn}} \approx 16\%$  in  $\text{TbMn}_2\text{Ge}_2$ ) decreases upon the transition of the manganese subsystem from the ferro- to the antiferromagnetic state in compounds of the system  $\text{Nd}_x\text{Tb}_{1-x}\text{Mn}_2\text{Ge}_2$  for  $x=0-0.4$ .

Magnetic studies have shown<sup>6,11,12,17,27</sup> that the axis of easy magnetization (EA) in  $\text{RMn}_2\text{Ge}_2$  compounds with  $\text{R}=\text{La}, \text{Pr}, \text{Gd}, \text{Tb}, \text{Dy}, \text{Ho},$  and  $\text{Tm}$  is oriented along the tetragonal axis, while in  $\text{ErMn}_2\text{Ge}_2$  the EA is parallel to the  $[110]$  direction.<sup>19,21</sup> In the compound  $\text{NdMn}_2\text{Ge}_2$  at temperatures above  $T_{sr}=250$  K the EA is the  $c$  axis, while for  $T < T_{sr}$  the EA is reoriented in the (001) plane,<sup>12</sup> so that a spin-reorientation phase transition occurs. In  $\text{SmMn}_2\text{Ge}_2$  at temperatures above  $T_t=100$  K the EA is parallel to the  $c$  axis, and for  $T < T_t$  the EA is oriented along the  $[110]$  axis.<sup>13</sup>

The magnetization curves of  $\text{RMn}_2\text{Ge}_2$  single crystals along the easy and hard magnetization directions show<sup>19</sup> that compounds in which the rare earth atoms have a nonzero orbital moment have a large magnetic anisotropy (Table II). It is seen from the table that the magnetic anisotropy of  $\text{GdMn}_2\text{Ge}_2$  (the  $\text{Gd}^{3+}$  ion is found in an  $S$  state) is an order

TABLE II. Values of the magnetic anisotropy constants of  $\text{RMn}_2\text{Ge}_2$  compounds at  $T=4.2$  K (according to the data of Refs. 11 and 19).

R	$K_1$ , erg/cm <sup>3</sup>	EA
La	$22 \cdot 10^6$	[001]
Pr	$53 \cdot 10^7$	[001]
Gd	$54 \cdot 10^6$	[001]
Tb	$84 \cdot 10^7$	[001]
Dy	$13 \cdot 10^8$	[001]
Ho	$13 \cdot 10^8$	[001]
Er	$-42 \cdot 10^8$	[110]

of magnitude smaller than the magnetic anisotropy of the other compounds with magnetic rare earths. This indicates that the large magnetic anisotropy is due to the rare earth ions and apparently, as in the other R–T intermetallides, has a single-ion nature.

#### 4. EXCHANGE INTERACTIONS IN $\text{RMn}_2\text{Ge}_2$ INTERMETALLIC COMPOUNDS

We have shown that the compounds  $\text{RMn}_2\text{Ge}_2$  have various magnetic structures, and various magnetic phase transitions occur in them as the temperature is varied. The formation of these structures and transitions is intimately related to the competition among the different types of exchange interactions, with the different mechanisms contributing to them (the RKKY exchange interaction via conduction electrons, and superexchange between the magnetic atoms via germanium). Generally speaking, the exchange interactions in the  $\text{RMn}_2\text{Ge}_2$  intermetallides can be divided into four classes:

- Mn–Mn in the layer;
- interlayer Mn–Mn (in the simplest case between nearest manganese planes);
- Mn–R;
- R–R.

Numerous studies have shown (see, e.g., the review<sup>1</sup>) that the strongest is the exchange interaction between Mn ions in the layer, which is mainly determined by the magnetic ordering temperature of the intermetallides  $\text{RMn}_2\text{Ge}_2$ . In compounds with heavy rare earths this interaction is ferromagnetic. In compounds with light rare earths an antiferromagnetic ordering arises in the layer at high temperatures (above  $T_C$ ). This is due to the onset of an antiferromagnetic component of the intralayer exchange, which depends on the Mn–Mn interatomic distance  $d_{\text{Mn–Mn}}$  in the layer. According to Ref. 26, the critical distance  $d_c$  is approximately 2.87 Å. In compounds with heavy rare earths one has  $d_c > d_{\text{Mn–Mn}}$ , and therefore in those intermetallides the antiferromagnetic component is absent, and the manganese in the layer is ordered ferromagnetically. In intermetallides with light rare earths, for which  $d_c < d_{\text{Mn–Mn}}$ , the antiferromagnetic compo-

ment of the exchange gives rise to an antiferromagnetic (collinear or noncollinear) magnetic ordering in the layer. We note, however, that the origin and features of the antiferromagnetic component of the exchange interaction in the layer has been insufficiently well studied and is in need of further investigation.

The exchange interaction between manganese planes is an order of magnitude smaller than the Mn–Mn exchange interaction in the layer. As has been shown by many authors (see, e.g., Ref. 13 and the references cited therein), this interaction is also strongly dependent on the Mn–Mn interatomic distance in the layer and changes sign at a certain critical value  $d_{c1} = 2.86 \text{ \AA}$ . In compounds with light rare earths the Mn–Mn interatomic distance at room temperature is larger than  $d_{c1}$ , and the exchange interaction between nearest manganese planes is ferromagnetic. In configurations with heavy rare earths, on the contrary, this interaction is antiferromagnetic, since the Mn–Mn interatomic distance is less than  $d_{c1}$ . As a result, in compounds with light rare earths the manganese subsystem has a ferromagnetic structure, and in intermetallides with heavy rare earths at temperatures above the magnetic ordering temperature of the rare earths the manganese subsystem is found in an antiferromagnetic state. The dependence of the manganese–manganese interplane exchange on the interatomic distance has been confirmed by numerous studies both on  $\text{SmMn}_2\text{Ge}_2$  and on several mixed compounds.<sup>25,29,30</sup> In  $\text{SmMn}_2\text{Ge}_2$  the Mn–Mn interatomic distance in the layer is close to  $d_{c1}$ . At room temperature  $d > d_{c1}$  in this compound, and  $\text{SmMn}_2\text{Ge}_2$  is a ferromagnet. On cooling, because of the change of the interatomic distances with temperature,  $d$  becomes smaller, and there is a transition of the manganese subsystem to an antiferromagnetic state on account of the change in sign of the Mn–Mn interlayer exchange interaction. Further decrease in temperature leads to magnetic ordering of the Sm subsystem, which induces a return of the ferromagnetic ordering of the manganese subsystem. An analogous transition of the manganese subsystem is observed in compounds with Gd, Tb, and Dy as the temperature is lowered to  $T_t$ .

We note that because of the dependence of the Mn–Mn interplane exchange interaction on the interatomic distance in the layer,  $d$  (or, in other words, on the crystal lattice parameter  $a$ ), appreciable magnetoelastic anomalies appear on the temperature dependence of the parameter  $a$  at the spontaneous magnetic phase transitions due to the transition of the manganese subsystem from the ferro- to the antiferromagnetic state.<sup>31</sup> This is clearly seen in Fig. 4, which shows the temperature dependence of the parameters of the crystal structure of several  $\text{RMn}_2\text{Ge}_2$  intermetallides from Ref. 31.

The Mn–R exchange interaction has approximately the same value as the exchange interaction between nearest manganese planes. The competition of these two interactions determines the magnetic properties of these compounds at low temperatures. In compounds with Gd, Tb, and Dy at the magnetic ordering temperature of the R subsystem, the Mn subsystem undergoes a transition from the antiferromagnetic to a ferromagnetic state on account of the fact that the Mn–R exchange interaction is larger than the antiferromagnetic exchange interaction between nearest manganese planes. In compounds with Ho, Er, and Tm the antiferromagnetism in

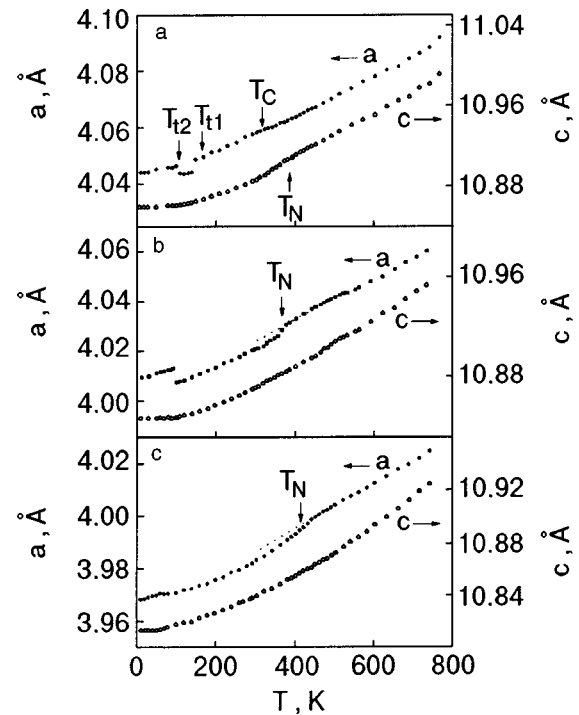


FIG. 4. Temperature dependence of the crystal structure parameters of the compounds  $\text{RMn}_2\text{Ge}_2$ : R = Sm (a), Gd (b), Dy (c).

the Mn subsystem persists to the lowest temperatures, since in these compounds the Mn–R exchange interaction is smaller than the manganese interplane exchange interaction. The magnetic ordering of the R subsystem in compounds with Gd, Tb, and Dy is due to the Mn–R exchange interaction, while in compounds with Ho, Er, and Tm the magnetic ordering of the R subsystem is caused by the R–R exchange interaction proper, which is an order of magnitude smaller than the Mn–R exchange interaction.

We conclude this Section by noting that the nature of the magnetism of a  $3d$  subsystem in intermetallides of the  $\text{RT}_2\text{X}_2$  type is unclear at the present time. In Refs. 32 and 33 an attempt was made to explain the difference of the properties of the manganese and other  $3d$  subsystems in these intermetallides in the framework of an itinerant magnetism model. The band structure of the intermetallides  $\text{LaMn}_2\text{Ge}_2$ ,  $\text{YMn}_2\text{Ge}_2$ , and  $\text{LaCo}_2\text{Ge}_2$  was calculated, and it was shown that the value of the density of states at the Fermi level in  $\text{YMn}_2\text{Ge}_2$  and  $\text{LaMn}_2\text{Ge}_2$  is relatively large, and the Stoner criterion for itinerant ferromagnetism is satisfied for those compounds. For  $\text{LaCo}_2\text{Ge}_2$  the density of states at the Fermi level is considerably smaller, and for that intermetallide the Stoner criterion is not satisfied, and therefore the Co subsystem is nonmagnetic. Thus calculations in a band model can explain the presence of magnetic ordering in the manganese subsystem and its absence in the cobalt subsystem of the compound  $\text{RT}_2\text{Ge}_2$ . However, analysis of the magnetic moments of the manganese in the magnetically ordered and paramagnetic states led the authors of Ref. 1 to conclude that the magnetism of the manganese subsystem in  $\text{RM}_2\text{Ge}_2$  intermetallides cannot be described completely in a band model. This question needs further investigation.

**5. DESCRIPTION OF THE MAGNETIC PROPERTIES OF RMn<sub>2</sub>Ge<sub>2</sub> INTERMETALLIDES IN THE YAFET–KITTEL MODEL FOR FERRIMAGNETS WITH AN ANTIFERROMAGNETIC INTRASUBLATTICE EXCHANGE INTERACTION**

Thus the RMn<sub>2</sub>Ge<sub>2</sub> intermetallic compounds have two magnetic sublattices: manganese and rare-earth. In the intermetallics with heavy rare earths the exchange interaction between these subsystems is antiferromagnetic, and therefore these intermetallics can be treated as two-sublattice ferrimagnets. An important feature of RMn<sub>2</sub>Ge<sub>2</sub> with heavy rare earths is that the exchange interaction between neighboring manganese layers is also antiferromagnetic, and these compounds can therefore be treated as two-sublattice ferrimagnets with an antiferromagnetic exchange interaction in one of the sublattices. The properties of these ferrimagnets were first calculated by Yafet and Kittel,<sup>34</sup> who showed that in the exchange approximation for  $H=0$  in addition to the ordinary collinear ferrimagnetic (Fi) phase, in which the magnetic moments of the sublattices are oriented antiparallel to each other, there can arise a triangular (T) magnetic phase in which the sublattice with the antiferromagnetic intrasublattice exchange interaction (the unstable sublattice) splits up into two equivalent subsublattices, the magnetic moments of which are oriented the same relative to the magnetic moment of the stable sublattice and at an angle to each other. Subsequently it was established<sup>35</sup> that in the presence of a field, such a ferrimagnet can have, besides the T phase, in which the magnetic moments of the sublattices are oriented at an angle to each other, and the ferromagnetic (F) phase, in which the magnetic moments of the sublattices are parallel to each other, an additional phase in which the magnetic moments of the subsublattices are antiparallel (an antiferromagnetic (AF) phase).

The Yafet–Kittel model has been used<sup>36–38</sup> to describe the properties of the intermetallics of the systems Gd<sub>1-x</sub>Y<sub>x</sub>Mn<sub>2</sub>Ge<sub>2</sub> and Gd<sub>1-x</sub>La<sub>x</sub>Mn<sub>2</sub>Ge<sub>2</sub>. For such systems the thermodynamic potential at low temperatures can be written in the form

$$\begin{aligned} \Phi = & -\lambda_{12}\mathbf{M}\cdot(\mathbf{m}_1+\mathbf{m}_2)-\lambda'_{22}\mathbf{m}_1\cdot\mathbf{m}_2-\frac{1}{2}\lambda_{22}(m_1^2+m_2^2) \\ & -\frac{1}{2}\lambda_{11}\mathbf{M}^2-\frac{K}{2m^2}(m_{1z}^2+m_{2z}^2)-H(\mathbf{M}+\mathbf{m}_1+\mathbf{m}_2). \end{aligned} \tag{1}$$

Here the first term describes the exchange interaction of the stable (magnetic moment  $\mathbf{M}$ ) and unstable (magnetic moment  $\mathbf{m}_1+\mathbf{m}_2$ ) sublattices ( $\lambda_{12}<0$ ), the second term describes the exchange between the sublattices ( $\lambda'_{22}<0$ ), the third the exchange within the sublattices ( $\lambda_{22}>0$ ), the fourth the exchange interaction within the stable sublattice ( $\lambda_{11}>0$ ), the fifth the magnetic anisotropy of the unstable sublattice (the  $z$  axis coincides with the axis of the crystal,  $m=|\mathbf{m}_1|=|\mathbf{m}_2|$ ), and the last term describes the Zeeman energy. We emphasize that in this case the nearest-neighbor approximation is used, i.e., only the exchange interactions of neighboring planes of a given type are taken into account. In systems with gadolinium, which is an  $S$  ion, one can neglect the magnetic anisotropy of the gadolinium subsystem (the

case of a non- $S$  ion is analyzed in the next Section) and assume that only the unstable manganese sublattice has anisotropy, and for it the direction of easy magnetization, according to the experimental data, is parallel to the axis of the crystal (magnetic anisotropy constant  $K>0$ ) for the systems under study.

From the conditions of minimum thermodynamic potential one can determine the equilibrium magnetic structures and construct the magnetic phase diagrams and magnetization curves. It follows from the thermodynamic potential (1) that (see Ref. 36 for more details) in the absence of field this system, for a sufficiently strong intersublattice exchange interaction, will go to a collinear Fi phase with the magnetic moments of the sublattices directed collinearly with the axis of the crystal. Decreasing the intersublattice exchange will lead to a second-order transition from the Fi phase to the triangular T phase, with an orientation of the magnetic moment of the stable sublattice parallel to the axis of the crystal. Upon further decrease of the exchange interaction between sublattices, the magnetic moment of the stable sublattice undergoes a jumplike reorientation to a direction perpendicular to the axis of the crystal, and a new triangular phase T' arises. Finally, if the exchange field acting on the unstable sublattice is equal to zero, then an antiferromagnetic structure arises in that sublattice, with an orientation of the magnetic moments of the subsublattices collinear with the axis of the crystal. The spontaneous magnetic structures arising in a two-sublattice ferrimagnet with negative exchange in one of the sublattices and uniaxial anisotropy in that sublattice are shown in Fig. 5.

Thus in the presence of anisotropy of the unstable sublattice, the triangular structure that was shown by Yafet and Kittel to arise in an isotropic ferrimagnet with magnetic instability will split up into two triangular structures with a perpendicular orientation of the magnetic moment of the stable sublattice. The transition from phase T to T' is due to the fact that in the T phase a decrease of the intersublattice exchange will lead to a decrease of the angle between the axis of the crystal and the directions of the magnetic moments of the subsublattices, causing an increase in the magnetic anisotropy energy and stimulating a transition to the T' phase, in which the magnetic anisotropy energy decreases.

Let us now analyze the behavior of an anisotropic ferrimagnet with magnetic instability in a magnetic field. We consider the situation in which the magnetic moment of the stable sublattice is greater than the magnetic moment of the unstable sublattice. For simplicity we limit consideration to the case when the total moment of the crystal in the initial

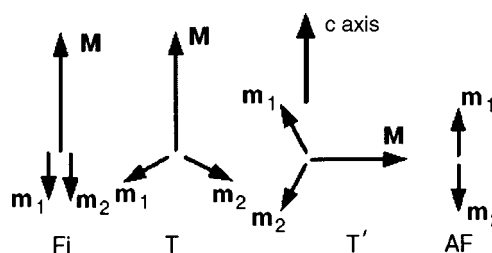


FIG. 5. Possible spontaneous magnetic phases of a ferrimagnet with an antiferromagnetic exchange interaction in the unstable sublattice with allowance for the magnetic anisotropy of that sublattice.

state is oriented along the axis of the crystal (phases Fi and T) and the external field is also directed along that axis. Then the problem reduces to finding the behavior of a uniaxial antiferromagnet in an effective field equal to the sum of the external field and the molecular field acting on the unstable sublattice on account of the stable sublattice. If  $M > 2m$  then for a comparatively small magnetic anisotropy ( $K < -2\lambda'_{22}m$ ) the following sequence of phases arises with increasing field:  $Fi \leftrightarrow T \leftrightarrow AF \leftrightarrow T \leftrightarrow F$ . The transitions between the triangular and antiferromagnetic phases is first-order, and the rest are second-order magnetic phase transitions. The magnetization curve in this case is shown schematically in Fig. 6, and the transition fields are as follows:

$$\begin{aligned} H_{Fi \leftrightarrow T} &= 2\lambda'_{22}m - \lambda_{12}M + 2K, \\ H_{T \leftrightarrow AF} &= -\lambda_{12}M - \sqrt{(-2\lambda'_{22}m^2 + K)K}, \\ H_{AF \leftrightarrow T} &= -\lambda_{12}M + \sqrt{(-2\lambda'_{22}m^2 + K)K}, \\ H_{T \leftrightarrow F} &= -2\lambda'_{22}m - \lambda_{12}M - 2K. \end{aligned} \tag{2}$$

If the magnetic anisotropy constant increases, then for  $K > -2\lambda'_{22}m$  the canted phases become energetically unfavorable—the system becomes Ising-like.

For a field orientation perpendicular to the axis of the crystal, the following sequence of phases is realized at fields higher than the technical saturation field (when the magnetic moment of the stable sublattice is oriented perpendicular to the axis of the crystal):  $Fi' \leftrightarrow T' \leftrightarrow F'$  (the prime indicates that the magnetic moment of the stable lattice is oriented perpendicular to the axis of the crystal). The critical fields for these second-order transitions are described by the expression

$$H = -\lambda_{12}M \pm \lambda'_{22}m \left( 2 - \frac{K}{\lambda'_{22}m^2} \right),$$

where the plus sign pertains to the transition  $Fi' \leftrightarrow T'$  and the minus sign to  $T' \leftrightarrow F'$ . We note, however, that the ferrimag-

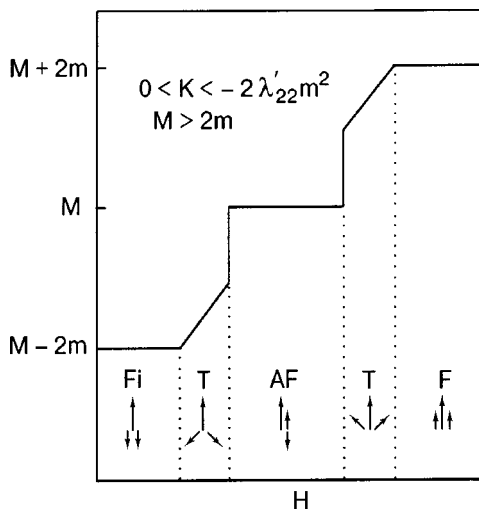


FIG. 6. Magnetization curve of an anisotropic ferrimagnet with an antiferromagnetic exchange interaction in the unstable sublattice in a field along the axis of the crystal.

netic structure does not arise if the technical saturation field is larger than the critical field of the transition  $Fi' \leftrightarrow T'$  (Ref. 36).

We should point out that the formulas presented above pertain to low temperatures, where the field dependence of the magnetic moments of the stable and unstable sublattices do not need to be taken into account. At higher temperatures, where the field dependence of these moments must not be neglected, the calculation is done numerically (see Refs. 36, 38, and 39). For this the free energy of the different phases is calculated with both the internal energy and the entropy contribution taken into account, and the phase with the minimum free energy under the given conditions is found.

We recall that in the calculations it is necessary to take into account the strong dependence of the Mn–Mn interplane exchange interaction (the parameter  $\lambda'_{22}$ ) on the interatomic distances in the plane (or on the lattice parameter  $a$ ). This effect leads to a dependence of  $\lambda'_{22}$  on the temperature and concentration and in a number of cases can have a substantial influence on the magnetic properties. If it is assumed that the dependence  $\lambda'_{22}(a)$  is linear,

$$\lambda'_{22} = \rho(a - a_c)$$

( $a_c = 4.045 \text{ \AA}$  for  $\text{RMn}_2\text{Ge}_2$ ), then this effect can be taken into account in the framework of the Kittel exchange inversion model.<sup>40</sup> (This question is discussed in more detail in Refs. 37 and 38.)

The approximation described above was used to analyze the experimental data for the system of intermetallides  $\text{Gd}_{1-x}\text{Y}_x\text{Mn}_2\text{Ge}_2$  (Ref. 36). Replacing gadolinium with yttrium leads to a decrease of the magnetic moment of the stable (gadolinium) sublattice and thereby decreases the molecular field acting on the unstable (manganese) on account of the stable sublattice and thus alters the ground state of the unstable sublattice. It should be noted that the concept of a “stable” gadolinium sublattice must be employed with some caution, since replacing even a small amount of the gadolinium with yttrium can alter the character of the long-range exchange in the spin subsystem of gadolinium and lead to the formation of new magnetic phases.<sup>41</sup> In the present case, however, the details of the interactions in the Gd sublattice are overwhelmed by the stronger intersublattice interaction, and the gadolinium subsystem can be regarded as stable.

The measurements<sup>36</sup> were made on “free” powders, the particles of which could rotate in an external field. It was shown that at all of the concentrations studied ( $0 \leq x \leq 0.5$ ) the samples had a spontaneous magnetization at low temperatures and underwent a metamagnetic transition in a field (Fig. 7).

The temperature dependence of the magnetization of the gadolinium–yttrium intermetallides is shown in Fig. 8. These compounds can be divided into three groups according to the character of the curves. The magnetization of compounds with a low yttrium concentration ( $x = 0, 0.1, 0.2$ ) decreases monotonically with increasing temperature before falling off sharply after a certain temperature  $T_1$  is reached. In the compounds with  $x = 0.3$  and  $0.4$  the magnetization varies weakly at low temperatures, then increases sharply after a certain temperature  $T_2$  is reached; this is followed by a monotonic decrease up to a temperature  $T_3$ , above which the magneti-

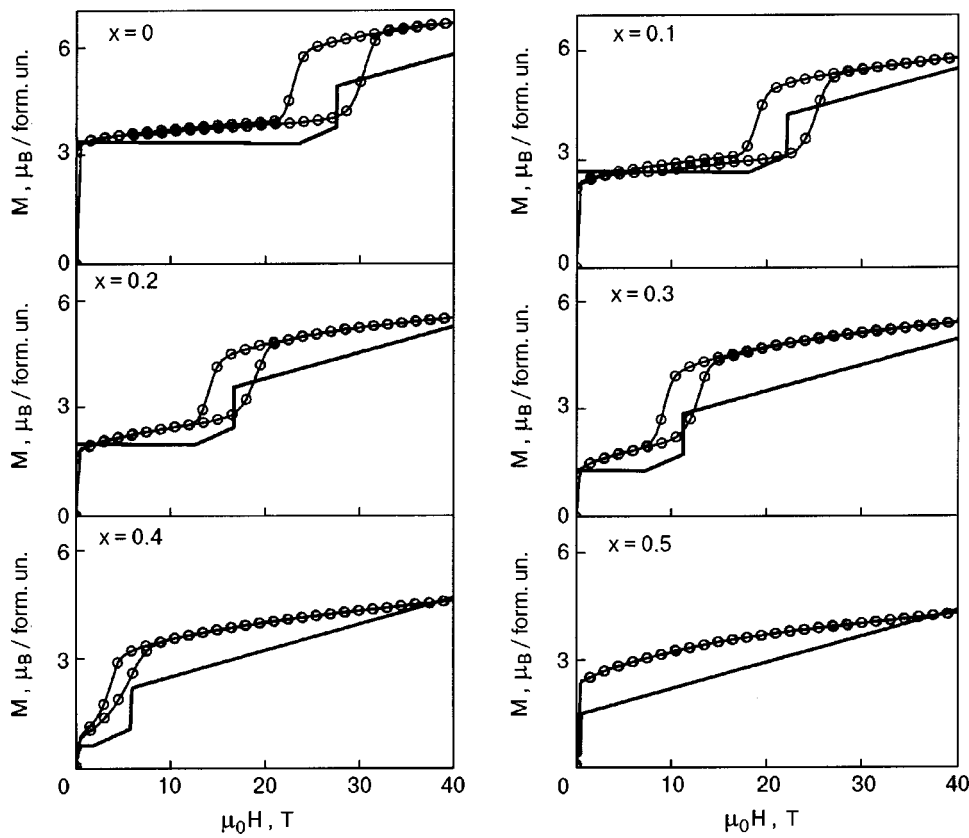


FIG. 7. Magnetization curves for free powders of the intermetallides  $Gd_{1-x}Y_xMn_2Ge_2$  at 4.2 K. The points are experimental data, and the curves are calculated.

zation depends weakly on temperature. Finally, for  $x=0.5$  the magnetization falls off monotonically with increasing temperature. Analysis of the magnetic data and the results of x-ray diffraction measurements of the crystal structure parameters of these compounds show that the transitions at

temperatures  $T_1$  and  $T_2$  are first-order magnetic phase transitions, while that at  $T_3$  is a second-order phase transition. Above  $T_c$  a weak magnetic state is observed at all the concentrations studied. The  $T-x$  magnetic phase diagram of the intermetallides  $Gd_{1-x}Y_xMn_2Ge_2$  is shown in Fig. 9.

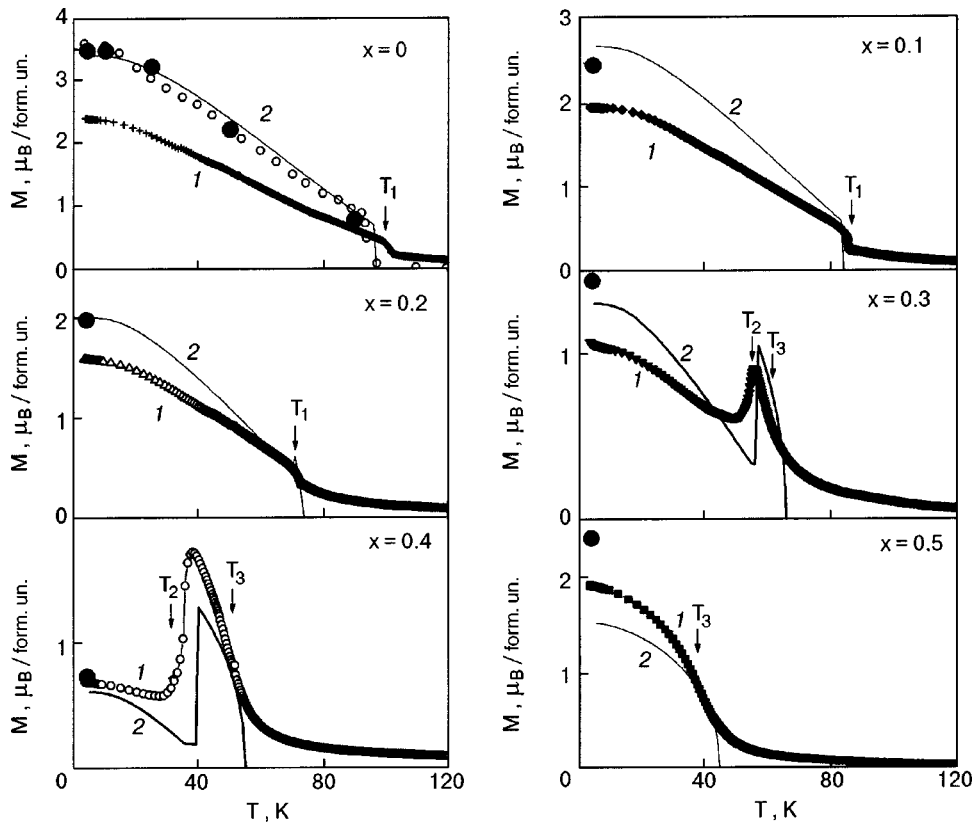


FIG. 8. Temperature dependence of the magnetization of  $Gd_{1-x}Y_xMn_2Ge_2$  intermetallides: experimental data in a field of 0.83 T for free powders (1); theoretical dependences (2); ●—values of the spontaneous magnetization obtained from measurements in high magnetic fields (see Fig. 7). For the compound with  $x=0$  the spontaneous magnetization data of Ref. 27 for a single crystal are also shown (○);  $T_i$  are the critical temperatures of the phase transitions.

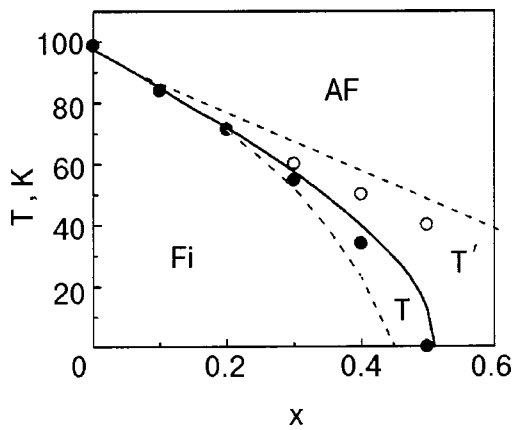


FIG. 9. Magnetic  $T$ - $x$  phase diagram for  $\text{Gd}_{1-x}\text{Y}_x\text{Mn}_2\text{Ge}_2$  intermetallides:  $\circ$ ,  $\bullet$ —experimental data for second- and first-order phase transitions, respectively. The calculated phase diagrams are shown by the dashed (second-order transition) and solid (first-order transition) curves.

The experimental data can be explained in terms of a modified Yafet–Kittel model in the following way. At low temperatures the gadolinium-rich compounds ( $x \leq 0.4$ ) have a rather large intersublattice exchange interaction. This leads to ferromagnetic ordering of the manganese subsystem and, consequently, those intermetallides are collinear ferrimagnets. At  $x=0.5$  the intrasublattice exchange interaction is insufficient for collinear ferromagnetic ordering of the unstable manganese subsystem—the triangular phase appears, and the total moment increases (see Fig. 8). As the temperature is raised, the decrease in the magnetization of the gadolinium subsystem leads to a decrease in the molecular field acting on the unstable manganese subsystem, and in compounds with  $x=0, 0.1$ , and  $0.2$  this subsystem undergoes a transition to an antiferromagnetic state at a temperature  $T_1$ , and the gadolinium subsystem becomes paramagnetic. We note that this behavior has been confirmed previously for a number of  $\text{RMn}_2\text{Ge}_2$  intermetallides by neutron diffraction studies.<sup>1,10</sup> In compounds with  $x=0.3$  and  $0.4$  there is a second-order transition from the Fi phase to the T phase on heating and then, as the temperature is increased further to  $T_2$  there is a second-order transition from that phase to a triangular phase  $T'$ ; here the magnetization increases in a jump (the compound with  $x=0.5$  is already in the  $T'$  phase at 4.2 K, and therefore the second-order transition is absent). Finally, at a temperature  $T_3$  the manganese subsystem becomes antiferromagnetic while the gadolinium subsystem goes to a paramagnetic state.

The modified Yafet–Kittel model can also describe the metamagnetic transition observed in the free powders at high magnetic fields (Fig. 7). In Ref. 36 it was shown that the following sequence of phases should be observed in free powders with increasing field:  $\text{Fi} \leftrightarrow \text{T} \leftrightarrow \text{T}' \leftrightarrow \text{T} \leftrightarrow \text{F}$ , and that the transitions between triangular phases are first-order phase transitions while the rest are second-order. It can be assumed that the metamagnetic transition is due to a transition from the phase T to  $T'$ .

The modified Yafet–Kittel model is capable of not only a qualitative but also a quantitative description of the experimental data for the  $\text{Gd}_{1-x}\text{Y}_x\text{Mn}_2\text{Ge}_2$  intermetallides. The theoretical curves calculated in this model are shown by the

curves in Figs. 7–9. In the theoretical calculations the necessary exchange parameters are determined from the concentration dependence of the field of the metamagnetic transition at 4.2 K in the system  $\text{Gd}_{1-x}\text{Y}_x\text{Mn}_2\text{Ge}_2$  and from the temperatures of the spontaneous magnetic phase transitions and Néel temperature in  $\text{GdMn}_2\text{Ge}_2$ . The magnetic anisotropy constant  $K$  was determined from data on the field dependence of the magnetization of the  $\text{GdMn}_2\text{Ge}_2$  single crystal along the axis of hard magnetization at 4.2 K from Ref. 18 (the details of the calculation are given in Ref. 36):  $\lambda_{12} = -7.7 \text{ T}/\mu_B$ ,  $\lambda'_{22} = -10.9 \text{ T}/\mu_B$ ,  $\lambda_{22} = 245 \text{ T}/\mu_B$ ,  $\lambda_{11} = 2.2 \text{ T}/\mu_B$ , and  $K = 15.8 \text{ T} \cdot \mu_B$ . These parameters were also used in calculating the magnetization curves of the  $\text{GdMn}_2\text{Ge}_2$  single crystal for comparison with the experimental data (Figs. 10 and 11). It may be seen that the agreement of the theory with experiment is quite good.

Since the sizes of the Gd and Y atoms are close to each other, in analyzing the magnetic properties of  $\text{Gd}_{1-x}\text{Y}_x\text{Mn}_2\text{Ge}_2$  one can in a first approximation ignore the dependence of the exchange interaction between neighboring Mn planes on the concentration  $x$ . In contrast to the system with yttrium, in the intermetallides  $\text{Gd}_{1-x}\text{La}_x\text{Mn}_2\text{Ge}_2$  the concentration dependence of the interatomic distances is extremely large, since the atomic radii of Gd and La are very different. Therefore the magnetic properties of the yttrium- and lanthanum-substituted intermetallides of gadolinium are qualitatively different. However, in spite of this, a rather good description of the experimental data on the magnetization and magnetic phase diagrams of the  $\text{Gd}_{1-x}\text{La}_x\text{Mn}_2\text{Ge}_2$  system can be achieved using the data obtained for the gadolinium–yttrium intermetallides, if the dependence of the Mn–Mn interlayer exchange interaction on the interatomic distances is taken into account.<sup>37,38</sup>

In Fig. 12 the experimental temperature dependence of the magnetization of  $\text{Gd}_{1-x}\text{La}_x\text{Mn}_2\text{Ge}_2$  is compared with the dependence calculated in the Yafet–Kittel model. It is seen that satisfactory agreement is obtained between the theoretical and experimental data and, most importantly, that the theoretical model describes well the sequence of spontaneous transitions  $\text{Fi} \rightarrow \text{AF} \rightarrow \text{Fi} \rightarrow \text{paramagnetic phase (P)}$  observed experimentally at high temperatures in compounds with  $x < 0.1$ . The  $\text{Fi} \rightarrow \text{AF}$  transition is due to the fact that at higher temperatures the magnetic moment of the gadolinium subsystem decreases, and at the temperature of this transition the manganese subsystem goes to an antiferromagnetic state, while the gadolinium subsystem becomes paramagnetic. On further increase in temperature the crystal lattice parameter  $a$  increases on account of thermal expansion, and at the temperature of the reentrant transition  $\text{AF} \leftrightarrow \text{Fi}$  the interplane exchange interaction becomes ferromagnetic. We note that for  $x > 0.1$  this interaction is ferromagnetic in the entire temperature range ( $a > a_c$ ), and the intermetallides with such a La concentration behave as ordinary ferrimagnets. A comparison of the theoretical and experimental  $T$ - $x$  phase diagrams (Fig. 13) attests to their good agreement.

Thus the modified Yafet–Kittel model permits description of the magnetic properties of the mixed intermetallides over a wide range of concentrations and temperatures in the region of moderately high magnetic fields. We agree, though, that this is a simplified model, since it includes only the

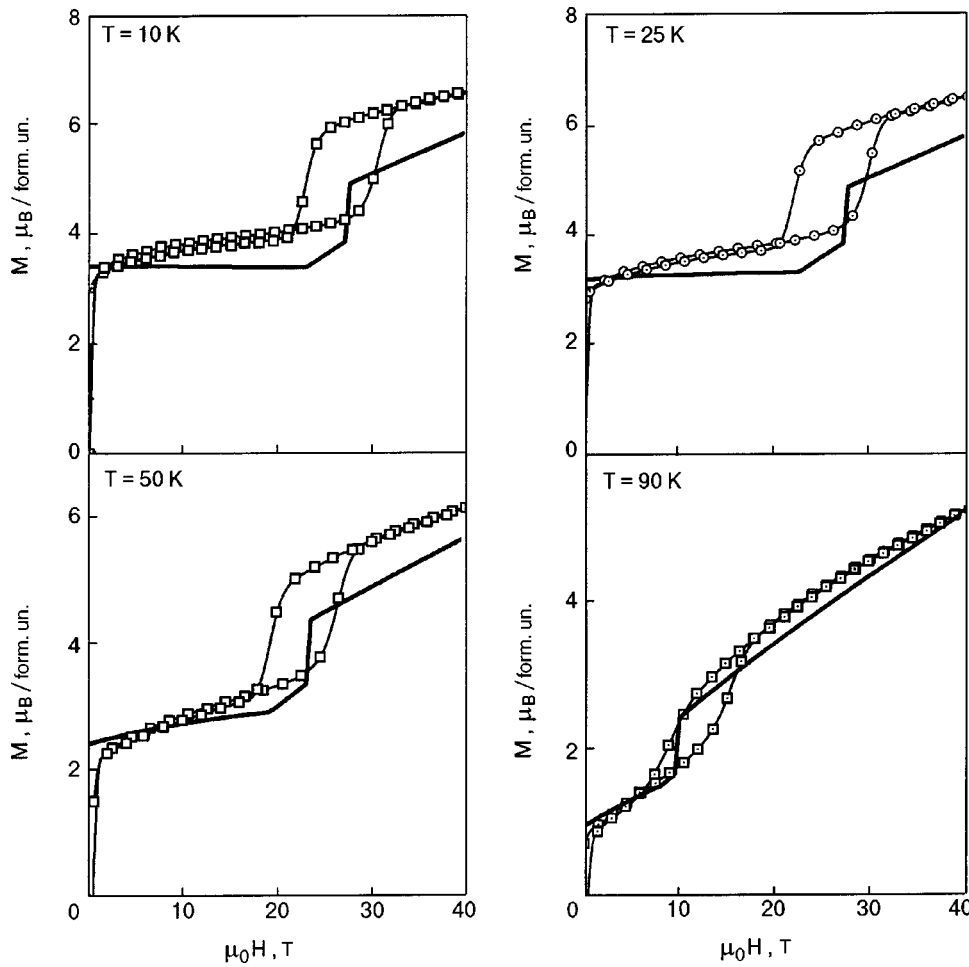


FIG. 10. Field dependence of the magnetization of  $\text{GdMn}_2\text{Ge}_2$  intermetallics for different temperatures. The symbols are experimental data, and the curves are calculated.

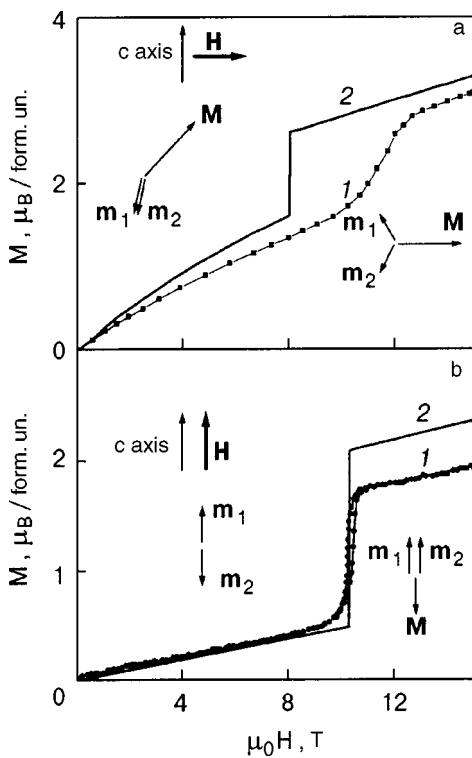


FIG. 11. Experimental (1), for a single crystal from Ref. 18, and calculated (2) magnetization curves of the intermetallic compound  $\text{GdMn}_2\text{Ge}_2$  at 77 K for  $\mathbf{H} \perp \mathbf{c}$  (a) and at 290 K for  $\mathbf{H} \parallel \mathbf{c}$  (b).

exchange interactions in the planes and between nearest-neighbor planes. It is incapable of describing the long-period magnetic structures observed in the  $\text{RMn}_2\text{Ge}_2$  intermetallics with light rare earths. Difficulties arise in using this model to describe the magnetic phase diagram of the  $\text{GdMn}_2\text{Ge}_2$  single crystal in high magnetic fields, etc. For this reason we have attempted to complicate the model and move beyond the framework of the Yafet–Kittel approximation in interpreting the magnetic properties of these intermetallics.

### 6. BEYOND THE YAFET–KITTEL APPROXIMATION

Yet another example of a shortcoming of the model set forth in the preceding Section, as an analysis of the available experimental data shows, is its inability to give even a qualitative description of the magnetic properties of the compound  $\text{DyMn}_2\text{Ge}_2$ . Magnetic and neutron diffraction studies on the single crystal have shown<sup>24</sup> that in  $\text{DyMn}_2\text{Ge}_2$  the magnetic moments of Mn order antiferromagnetically at  $T_N = 431$  K. According to the data of Ref. 24 and also of Refs. 22 and 43, where neutron diffraction studies were done on powders, in the low-temperature region  $\text{DyMn}_2\text{Ge}_2$  has two first-order magnetic phase transitions: at a temperature  $T_1$ , which according to the data of these studies lies in the interval from 33 to 35 K, and at  $T_2$ , from 37.5 to 40 K. For  $T < T_1$   $\text{DyMn}_2\text{Ge}_2$  is characterized by an Fi structure, analogous to that described above for  $\text{GdMn}_2\text{Ge}_2$ . For  $T > T_2$  the compound has an AF structure with disordered dysprosium

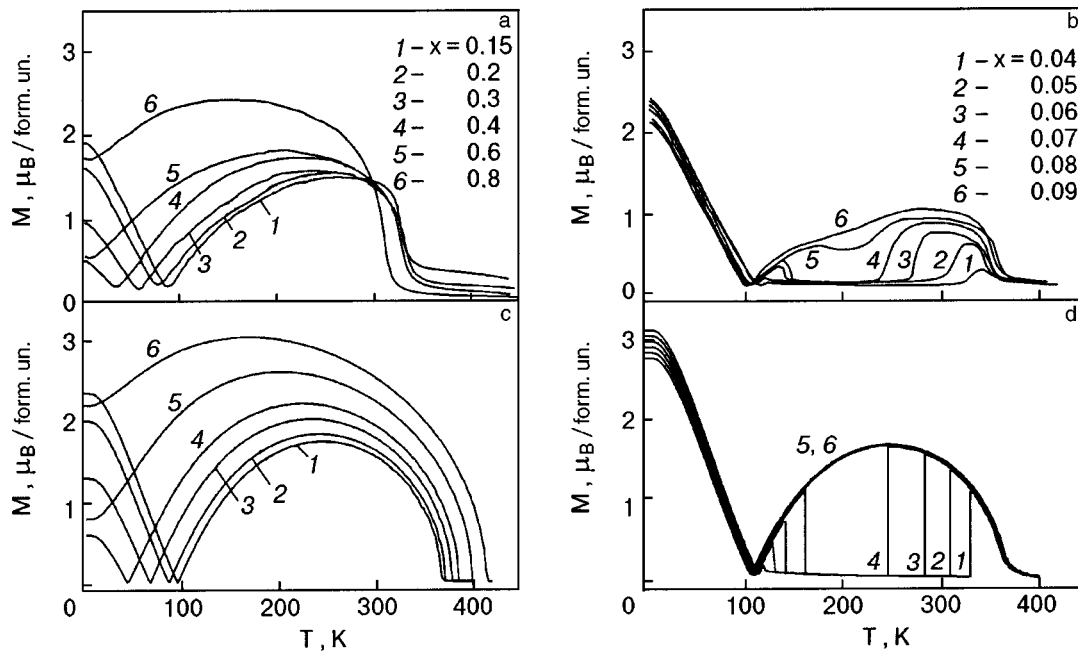


FIG. 12. Experimental (a,b) and theoretical (c,d) temperature dependence of the magnetization of  $Gd_{1-x}La_xMn_2Ge_2$  intermetallides.

moments. For the temperature interval between  $T_1$  and  $T_2$  the data of Refs. 22, 24, and 43 are inconsistent. According to Ref. 22, three phases coexist in this interval: Fi, I and AF

(see Fig. 3), and the magnetic unit cell is characterized by a tripling along the tetragonal axis, i.e.,  $a' = a$  and  $c' = 3c$ . According to Ref. 43, below  $T_2$  the AF phase does not exist, as can be seen from the temperature dependence of the integrated intensity of the corresponding line. The authors of Ref. 43 believe that a single incommensurate phase exists between  $T_1$  and  $T_2$ , with a wave vector  $\mathbf{k} \approx (0,0,0.65)$  according to a preliminary determination. The measurements of the magnetization curves on  $DyMn_2Ge_2$  single crystals in fields up to 15 T (Ref. 24) and 5 T (Ref. 44) have revealed the presence of first-order transitions in all of the investigated temperature range, up to 70 K.

The model described above is incapable, in particular, of explaining the existence of the magnetic structure observed in the temperature interval between  $T_1$  and  $T_2$ , the value of the jump in magnetization at the second-order phase transition at low temperatures in a field oriented along the tetragonal axis of the crystal,<sup>24</sup> etc. Therefore in Ref. 45 the model was refined to include the exchange interactions between the next-nearest magnetic layers. This is a natural refinement, since the exchange interaction in the intermetallides under study is brought about not only by the superexchange via germanium but also via conduction electrons, and it is long-ranged. The  $Dy^{3+}$  ion, in contrast to  $Gd^{3+}$ , is not an  $S$  ion, and so there will be substantial crystal-field effects. When these factors are taken into account, nonequivalent positions of the magnetic moments can arise in the crystal, both in the dysprosium and manganese magnetic subsystems. The presence of these nonequivalent positions and the exchange interactions between different layers of magnetic atoms were taken into account in writing the effective Hamiltonians in Ref. 45.

The effective Hamiltonian for the  $Dy^{3+}$  ion located in the  $i$ th position can be written in the molecular field approximation as

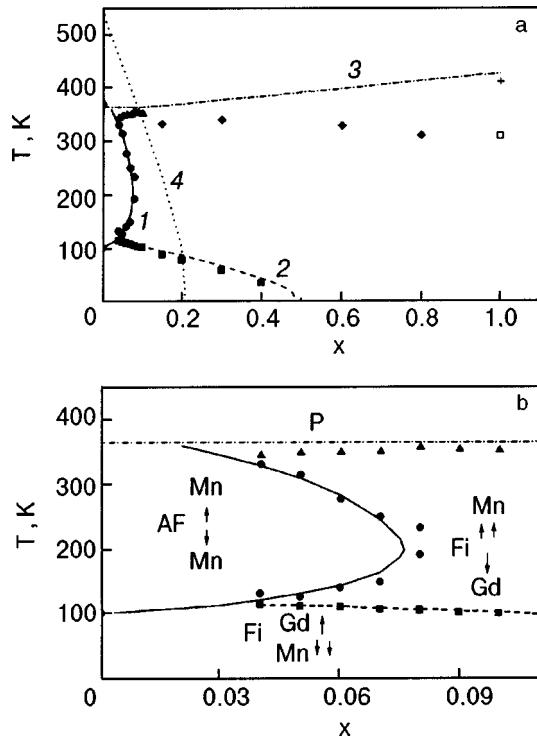


FIG. 13. a—The  $T$ - $x$  magnetic phase diagram of the  $Gd_{1-x}La_xMn_2Ge_2$  intermetallides in a field of 0.8 T (the points are experimental data, the curves are calculated): first-order phase transition  $Fi \leftrightarrow AF$  ( $\bullet$ ,  $J$ ); magnetic compensation temperature ( $\blacksquare$ , 2); the second-order transition to the paramagnetic state (Néel temperature  $T_N$ ) (3); temperature of the destruction of ferromagnetic order (the Curie temperature  $T_C$ ) ( $\blacktriangle$ ,  $\blacklozenge$ ); the line of the change of sign of the Mn–Mn interlayer exchange interaction (4); the temperatures  $T_N$  and  $T_C$  are from Ref. 8 ( $+$ ,  $\square$ ). b—The experimental part of the phase diagram from Ref. 42 for  $x < 0.1$  in comparison with the results of the calculation.

$$\begin{aligned} \mathcal{H}_{\text{Dy}}^{(i)} = & B_2^0 O_2^0 + B_4^0 O_4^0 + B_4^4 O_4^4 + B_6^0 O_6^0 \\ & + B_6^4 O_6^4 - g_J \mu_B \mathbf{J}^{(i)} (\mathbf{H} + \mathbf{H}_m^{(i)}), \end{aligned} \quad (4)$$

where  $B_n^m$  are the parameters of the crystalline field of tetragonal symmetry,  $O_n^m$  are equivalent operators,  $g_J$  is the Landé factor, and  $\mathbf{J}^{(i)}$  is the angular momentum operator of the  $\text{Dy}^{3+}$  ion. The molecular field  $\mathbf{H}_m^{(i)}$  is given by the expression

$$H_{mj}^{(i)} = \sum_l \lambda_{11}^{(l)} M_j^{(l)} + \sum_k \lambda_{12}^{(k)} m_j^{(k)}, \quad j = x, y, z. \quad (5)$$

The components of the  $i$ th dysprosium magnetic moment  $\mathbf{M}^{(i)}$  and the  $k$ th manganese magnetic moment  $\mathbf{m}^{(k)}$  are given by  $M_j^{(i)} = \mu_B g_J \langle J_j^{(i)} \rangle$  and  $m_j^{(k)} = \mu_B g \langle S_j^{(k)} \rangle$ , where  $g$  is the  $g$  factor of Mn,  $\mathbf{S}^{(k)}$  is the spin angular momentum operator of Mn, and  $\lambda_{11}^{(l)}$  and  $\lambda_{12}^{(k)}$  are the parameters of the Dy–Dy and Dy–Mn exchange interactions, respectively. The parameters of the Dy–Dy and Dy–Mn exchange interactions between atoms belonging to different layers appear in all the expressions additively,<sup>45</sup> and so it makes sense to use the summed parameters  $\lambda_{11}$  and  $\lambda_{12}$ .

For the  $k$ th magnetic moment of the  $d$  subsystem of manganese the effective Hamiltonian  $\mathcal{H}_{\text{Mn}}^{(k)}$  in the molecular field approximation with only the exchange interactions taken into account is equal to

$$\mathcal{H}_{\text{Mn}}^{(k)} = -g \mu_B \mathbf{S}^{(k)} \mathbf{H}_{\text{Mn}}^{(k)}. \quad (6)$$

The effective field acting on the  $k$ th magnetic moment of the Mn subsystem in an external magnetic field  $\mathbf{H}$  oriented at an angle  $\varphi$  to the  $c$  axis of the crystal is equal to

$$\begin{aligned} H_{\text{Mn}}^{(k)} = & H \cos(\varphi - \eta_k) + H_m^{(k)}, \\ H_m^{(k)} = & \sum_{n=k, k \pm 1, \dots} \lambda_{22}^{(n)} m^{(n)} \cos(\eta_n - \eta_k) \\ & + \lambda_{12} \sum_i (M_z^{(i)} \cos \eta_k + M_x^{(i)} \sin \eta_k), \end{aligned} \quad (7)$$

where  $\eta_k$  is the polar angle of the  $k$ th manganese moment, and  $\lambda_{22}^{(n)}$  are the parameters of the Mn–Mn exchange interaction between atoms belonging to the  $k$ th and  $n$ th layers. The anisotropy of the manganese subsystem, since it is small compared to the exchange, is included in the thermodynamic potential as an additive term.

The thermodynamic potential per formula unit in the molecular field approximation is given by the following expression ( $N$  is the number of nonequivalent formula units):

$$\begin{aligned} \Phi = & \frac{1}{N} \left\{ -k_B T \sum_{i=1}^N \ln Z_i + \frac{1}{2} \sum_{i=1}^N \mathbf{M}^{(i)} \mathbf{H}_m^{(i)} - k_B T \right. \\ & \times \sum_{k=1}^{2N} \ln \frac{\sinh[(2S+1)x_k/2]}{\sinh(x_k/2)} + \frac{1}{2} \sum_{k=1}^{2N} \mathbf{m}^{(k)} \mathbf{H}_m^{(k)} \\ & \left. + \sum_{k=1}^{2N} K \sin^2 \theta_k \right\}. \end{aligned} \quad (8)$$

The partition function  $Z_i$  for the  $i$ th dysprosium moment was calculated in Ref. 45 by numerical diagonalization of the Hamiltonian  $\mathcal{H}_{\text{Dy}}^{(i)}$  with the solution of the corresponding self-consistent problems,  $x_k = \mu_B g H_{\text{Mn}}^{(k)} / k_B T$ ; here and  $K$  is the

anisotropy constant for the manganese subsystem. The second and fourth terms in expression (8) are the usual correction terms in molecular field theory.

The problem of determining the set of parameters of the compound  $\text{DyMn}_2\text{Ge}_2$  when interpreting experimental data on the magnetic properties of this compound on the basis of the thermodynamic potential (8) was solved in Ref. 45.

At helium temperatures  $\text{DyMn}_2\text{Ge}_2$  has three first-order phase transitions from the initial phase Fi in a field along the tetragonal axis. At  $H \approx 7$  T a transition occurs to phase I, in which every third layer of the manganese subsystem has a magnetic moment reoriented along the field direction. The higher-field phases are the AF phase, with antiferromagnetic ordering in the manganese subsystem, and the F phase, in which the magnetic moments of both subsystems are oriented along the field. The values of the three critical fields are:  $H_{\text{Fi} \rightarrow \text{I}} = 7$  T,  $H_{\text{I} \rightarrow \text{AF}} = 32$  T, and  $H_{\text{AF} \rightarrow \text{F}} = 110$  T (Ref. 45) can be used to determine the three exchange parameters of the compound:  $\lambda_{12}$  (Dy–Mn),  $\lambda'_{22}$  (Mn–Mn in neighboring layers), and  $\lambda''_{22}$  (Mn–Mn in next-nearest layers). At low temperatures and high fields along the tetragonal axis the critical fields of these transitions are given by the expressions

$$\begin{aligned} H_{\text{Fi} \rightarrow \text{I}} = & -\lambda_{12} M + (\lambda'_{22} + \lambda''_{22}) m, \\ H_{\text{I} \rightarrow \text{AF}} = & -\lambda_{12} M + (\lambda'_{22} - 2\lambda''_{22}) m, \\ H_{\text{AF} \rightarrow \text{F}} = & -\lambda_{12} M - (\lambda'_{22} + \lambda''_{22}) m. \end{aligned} \quad (9)$$

For  $M = 10\mu_B$  and  $m = 2.2\mu_B$  (Ref. 24) the exchange parameters have the values  $\lambda_{12} = -5.85$  T/ $\mu_B$ ,  $\lambda'_{22} = -20$  T/ $\mu_B$ , and  $\lambda''_{22} = -3.5$  T/ $\mu_B$ . The total low-temperature magnetization curve calculated with these parameters for the compound  $\text{DyMn}_2\text{Ge}_2$  in the case when the field is applied along the tetragonal axis is shown in Fig. 14. Also shown there are the experimental curve measured in a field of up to 15 T in Ref. 24 and the high-field peaks of the differential magnetic susceptibility obtained in Ref. 45.

From the values of  $T_N = 440$  K and the known values of  $\lambda'_{22}$  and  $\lambda''_{22}$  one can find the parameter of the Mn–Mn exchange interaction in the layer:  $\lambda_{22} \approx 2 \times 10^3$  T/ $\mu_B$ . The  $H$ – $T$  phase diagram calculated on the basis of Eq. (8) is presented in Fig. 15 together with the experimental data obtained in Refs. 24, 44, and 45. We see that the calculated temperature dependence of the critical field  $H_{\text{Fi} \rightarrow \text{I}}$  is in good agreement with the experimental dependence obtained on a single crystal in Ref. 24. The field  $H_{\text{I} \rightarrow \text{AF}}$  according to the calculation depends more weakly on temperature than does that obtained from the measurements on free powders in Ref. 45. The extremely good agreement of the experimental<sup>24</sup> and calculated magnetization curves for the AF phase in a field parallel to the tetragonal axis can be seen in Fig. 16d.

For a field direction perpendicular to the tetragonal axis a first-order phase transition from the Fi to the triangular phase occurs at the critical field; in the triangular phase the magnetic moment of dysprosium is oriented along the field direction, while the Mn moments lie at obtuse angles to it. The corresponding theoretical magnetization curves calculated with the use of the crystal-field parameters determined in Ref. 45 ( $B_2^0 = 200$ ,  $B_4^0 = -3.5$ ,  $B_6^0 = -50$ , and  $B_4^4 = -390$  cm<sup>-1</sup>) are shown in Figs. 16a and 16b. It is seen that the calculated susceptibility in the Fi phase agrees with

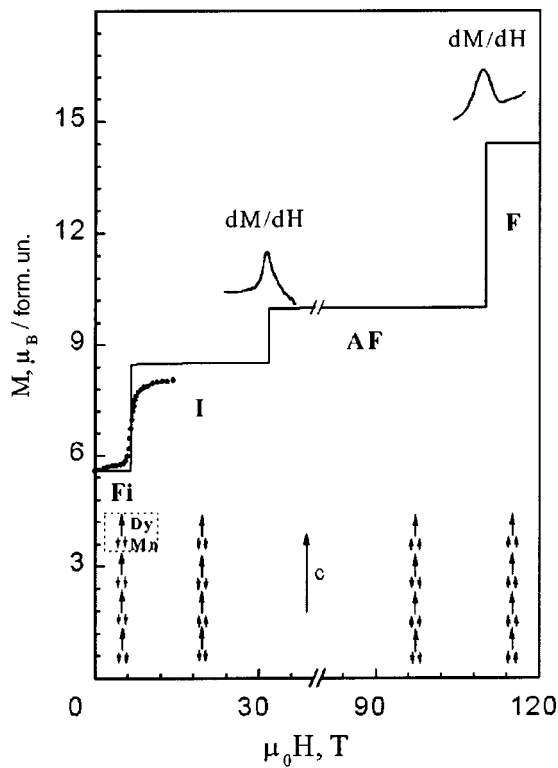


FIG. 14. Low-temperature magnetization of the compound  $\text{DyMn}_2\text{Ge}_2$  as a function of the field applied along the tetragonal axis. The curve is calculated, the filled circles are the experimental data for a single crystal at 4.2 K from Ref. 24. For the phase transitions  $\text{I} \leftrightarrow \text{AF}$  and  $\text{AF} \leftrightarrow \text{F}$  the peaks of  $dM/dH$  obtained in Ref. 45 for  $T=7$  and 5 K, respectively, are shown above the magnetization curve. The arrows indicate the magnetic moments of dysprosium and manganese in the layers. The dotted box encloses one formula unit.

the experimental dependence at both temperatures. The decrease of the critical field with increasing temperature is also correctly described (in both the experiment and theory the field of the phase transition is smaller at 20 K than at 4.2 K). The calculated jump in the magnetization is larger than that observed in experiment. Figures 16c and 16d show the magnetization curves for a field direction in the basal plane in the temperature region where the initial phase is AF. It is seen that at  $T=60$  K (Fig. 16c) the theoretical curve is in good

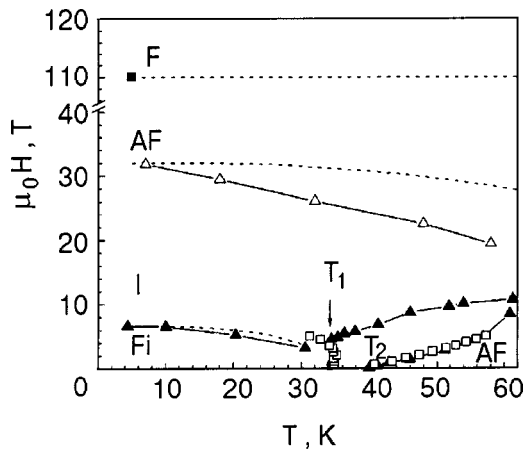


FIG. 15. Magnetic phase diagram  $H-T$  for  $\text{DyMn}_2\text{Ge}_2$ . The dashed curves are calculated, the rest is experimental data from Ref. 45 (■, △), Ref. 24 (▲), and Ref. 44 (□).

agreement with the experimental curve obtained in Ref. 44 in measurements on a single crystal in the form of a slab, with allowance for the demagnetizing fields. For  $T=77$  K (Fig. 16d) the agreement between the calculated and experimental (from Ref. 24) magnetization curves is poorer.

Thus when the exchange interaction between next-nearest manganese layers is taken into account together with the antiferromagnetic exchange interaction of nearest manganese layers, one can describe the magnetic properties of  $\text{DyMn}_2\text{Ge}_2$  over a wide range of magnetic fields.

We have attempted to apply this model to solve the problems of the first-order high-field transition in  $\text{GdMn}_2\text{Ge}_2$ . The second-order phase transition in  $\text{GdMn}_2\text{Ge}_2$  observed near 100 T in measurements of the differential magnetic susceptibility in ultrahigh magnetic fields<sup>46</sup> should be interpreted in the framework of the phase diagram of this compound for  $\mathbf{H} \parallel c$  as an  $\text{AF} \leftrightarrow \text{T}$  transition, since this is the only possible high-field first-order transition (see Fig. 6). The value of the critical field of this transition, calculated using the values determined for the parameters of  $\text{GdMn}_2\text{Ge}_2$  in the modified Yafet–Kittel model (see Sec. 5), came out to be  $\sim 70$  T, i.e., much less than the experimental value. This raises the question of whether the agreement of the experimental and calculated values of the field of this transition might be improved by taking into account the interaction between next-nearest Mn planes, as was the situation in the dysprosium compound. However, our calculations showed that the Mn–Mn exchange across an intervening layer does not appear in the expression for the critical fields of this phase diagram. This means that the problem requires further investigation.

### CONCLUSION

This review of the magnetic properties of layered intermetallic compounds  $\text{RMn}_2\text{Ge}_2$  has shown a great diversity of magnetic structures, magnetic phase diagrams, and various spontaneous and field-induced phase transitions in pure, diluted, and mixed compounds. It follows from an analysis of the magnetic properties of intermetallides with heavy rare earths that these compounds can be considered to be ferrimagnets with an antiferromagnetic exchange interaction in the manganese subsystem. In a number of cases their properties are satisfactorily described in the extremely simple model of a two-sublattice ferrimagnet with antiferromagnetic intrasublattice exchange (the Yafet–Kittel model) with allowance for the magnetic anisotropy. However, such a model is not always adequate, since it takes into account only the exchange interaction between nearest neighbors, and one must consider more complicated models. For example, for describing the properties of  $\text{DyMn}_2\text{Ge}_2$  it is necessary to take into account the exchange between next-nearest manganese layers. Apparently the antiferromagnetic component of the intraplane exchange interaction in the manganese subsystem is also important; it might make it possible to explain the long-period noncollinear magnetic structures observed in a number of  $\text{RMn}_2\text{Ge}_2$  intermetallides with light rare earths.

We note that  $\text{RMn}_2\text{Ge}_2$  compounds are natural superlattices, and some interesting questions concerning that property are beyond the scope of this review. In particular, there is an extremely significant giant magnetoresistance effect

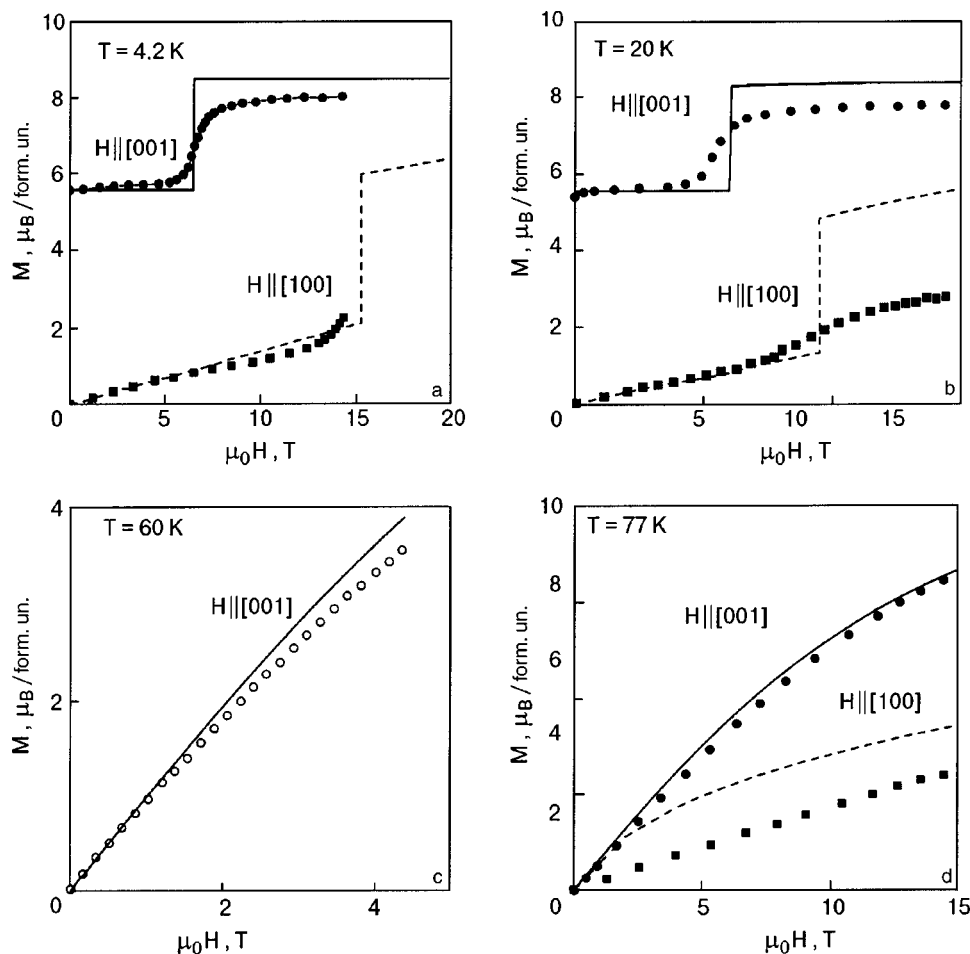


FIG. 16. Magnetization of the compound  $\text{DyMn}_2\text{Ge}_2$  as a function of magnetic field applied along the indicated directions for various temperatures  $T$  [K]: 4.2 (a), 20 (b), 60 (c), and 77 (d). The points are experimental data of Ref. 24 (●, ■) and Ref. 44 (○); the curves are calculated.

that is manifested at metamagnetic transitions induced by a magnetic field. In Refs. 47 and 48, for example, an unusually large (up to 15%) jump in the magnetoresistance in a field was observed in  $(\text{Gd}, \text{La})\text{Mn}_2\text{Ge}_2$  compounds near 200 K.

This study was supported by the Foundation for Support of Science Schools (Project No. 00-15-96695).

\*E-mail: levitin@plms.phys.msu.su

<sup>1</sup>A. Szytula and J. Leciejewicz, *Handbook on Physics and Chemistry of Rare Earths*, Vol. 12, edited by K. A. Gschneidner Jr. and L. Eyring, North Holland, Amsterdam (1989), p. 133.

<sup>2</sup>Z. Ban and M. Sikirica, *Acta Crystallogr.* **18**, 594 (1965).

<sup>3</sup>G. Venturini, *J. Alloys Compd.* **232**, 133 (1996).

<sup>4</sup>I. Nowik, Y. Levi, I. Felner, and E. R. Bauminger, *J. Magn. Magn. Mater.* **140–144**, 913 (1995); **147**, 373 (1995).

<sup>5</sup>K. S. V. L. Narashimhan, *J. Appl. Phys.* **46**, 4957 (1975).

<sup>6</sup>T. Shigeoka, N. Iwata, H. Fujii, and T. Okamoto, *J. Magn. Magn. Mater.* **53**, 83 (1985).

<sup>7</sup>A. Szytula and I. Szott, *Solid State Commun.* **40**, 199 (1981).

<sup>8</sup>G. Venturini, B. Malaman, and E. Ressouche, *J. Alloys Compd.* **241**, 135 (1996).

<sup>9</sup>G. Venturini, R. Welter, E. Ressouche, and B. Malaman, *J. Alloys Compd.* **210**, 213 (1994).

<sup>10</sup>R. Welter, G. Venturini, E. Ressouche, and B. Malaman, *J. Alloys Compd.* **218**, 204 (1995).

<sup>11</sup>N. Iwata, T. Ikeda, T. Shigeoka, H. Fujii, and T. Okamoto, *J. Magn. Magn. Mater.* **54–57**, 481 (1986).

<sup>12</sup>T. Shigeoka, N. Iwata, and H. Fujii, *J. Magn. Magn. Mater.* **76–77**, 189 (1988).

<sup>13</sup>H. Fujii, T. Okamoto, T. Shigeoka, and N. Iwata, *Solid State Commun.* **53**, 715 (1985).

<sup>14</sup>E. M. Gyorgy, B. Batlogg, J. P. Remeika, R. B. van Dover, R. M. Fleming, H. E. Blair, G. P. Espinosa, A. S. Cooper, and R. G. Maines, *J. Appl. Phys.* **61**, 4237 (1987).

<sup>15</sup>M. Duraj, R. Duraj, A. Szytula, and Z. Tomkowicz, *J. Magn. Magn. Mater.* **73**, 240 (1988).

<sup>16</sup>I. Felner and I. Nowik, *J. Phys. Chem. Solids* **39**, 763 (1978).

<sup>17</sup>T. Shigeoka, H. Fujii, H. Fujiwara, K. Yagasaki, and T. Okamoto, *J. Magn. Magn. Mater.* **31–34**, 209 (1983).

<sup>18</sup>H. Kobayashi, H. Onodera, and H. Yamamoto, *J. Magn. Magn. Mater.* **79**, 76 (1989).

<sup>19</sup>T. Shigeoka, *J. Sci. Hiroshima Univ.: Ser. A*, **48**, 103 (1984).

<sup>20</sup>J. Leciejewicz and A. Szytula, *Solid State Commun.* **49**, 361 (1984).

<sup>21</sup>G. Venturini, B. Malaman, and E. Ressouche, *J. Alloys Compd.* **240**, 139 (1996).

<sup>22</sup>G. Venturini, B. Malaman, K. Tomala, A. Szytula, and J. P. Sánchez, *Phys. Rev. B* **46**, 207 (1992).

<sup>23</sup>T. Ono, H. Onodera, M. Ohashi, H. Yamaguchi, and Y. Yamaguchi, *J. Magn. Magn. Mater.* **123**, 133 (1993).

<sup>24</sup>H. Kobayashi, H. Onodera, Y. Yamaguchi, and H. Yamamoto, *Phys. Rev. B* **43**, 728 (1991).

<sup>25</sup>Yin-gang Wang, Fuming Yang, Changpin Chen, N. Tang, and Qidong Wang, *J. Phys.: Condens. Matter* **9**, 8539 (1997).

<sup>26</sup>G. Venturini, R. Welter, E. Ressouche, and B. Malaman, *J. Magn. Magn. Mater.* **150**, 197 (1995).

<sup>27</sup>N. Iwata, K. Hattori, and T. Shigeoka, *J. Magn. Magn. Mater.* **53**, 318 (1986).

<sup>28</sup>L. Morellon, P. A. Algarabel, M. R. Ibarra, and C. Ritter, *Phys. Rev. B* **55**, 12363 (1997).

<sup>29</sup>M. Duraj, R. Duraj, and A. Szytula, *J. Magn. Magn. Mater.* **79**, 61 (1989).

<sup>30</sup>H. Fujii, M. Isoda, T. Okamoto, T. Shigeoka, and N. Iwata, *J. Magn. Magn. Mater.* **54–57**, 1345 (1986).

<sup>31</sup>I. Yu. Gaïdukova, Guo Guanghua, S. A. Granovskii, I. S. Dubenko, R. Z. Levitin, A. S. Markosyan, and V. E. Rodimov, *Fiz. Tverd. Tela (St. Petersburg)* **41**, 2053 (1999) [*Phys. Solid State* **41**, 1885 (1999)].

<sup>32</sup>S. Asano and J. Yamashita, *Prog. Theor. Phys.* **49**, 373 (1972).

<sup>33</sup>S. Ishida, S. Asano, and J. Ishifa, *J. Phys. Soc. Jpn.* **55**, 936 (1986).

- <sup>34</sup>Y. Yafet and C. Kittel, *Phys. Rev.* **87**, 290 (1952).
- <sup>35</sup>N. P. Kolmakova, S. A. Kolonogii, R. Z. Levitin, and H. W. Nekrasova, *Fiz. Tverd. Tela (St. Petersburg)* **41** 1797, (1999) [*Phys. Solid State* **41**, 1694 (1999)].
- <sup>36</sup>A. Yu. Sokolov, Guo Guanghua, S. A. Granovskii, R. Z. Levitin, Kh. Vada, M. Shiga, and T. Goto, *Zh. Éksp. Teor. Fiz.* **116**, 1346, (1999) [*JETP* **89**, 723 (1999)].
- <sup>37</sup>Guo Guanghua, R. Z. Levitin, V. V. Snegirev, D. A. Filippov, and A. Yu. Sokolov, *Zh. Éksp. Teor. Fiz.* **117**, 1127 (2000) [*JETP* **90**, 979 (2000)].
- <sup>38</sup>Guo Guanghua, R. Z. Levitin, A. Yu. Sokolov, V. V. Snegirev, and D. A. Filippov, *J. Magn. Magn. Mater.* **214**, 301 (2000).
- <sup>39</sup>Guo Guanghua, N. P. Kolmakova, R. Z. Levitin, M. Yu. Nekrasova, A. Yu. Sokolov, and D. A. Filippov, in *Proceedings of MISM'99 MSU, Moscow* (1999), part 2, p. 233.
- <sup>40</sup>C. Kittel, *Phys. Rev.* **120**, 335 (1960).
- <sup>41</sup>V. V. Eremenko, A. B. Beznosov, E. L. Fertman, P. P. Pal-Val, and V. P. Popov, *Adv. Cryog. Eng.* **46**, 413 (2000).
- <sup>42</sup>A. Sokolov, H. Wada, M. Shiga, and T. Goto, *Solid State Commun.* **105**, 289 (1998).
- <sup>43</sup>H. Kobayashi, M. Ohashi, H. Onodera, T. Ono, and Y. Yamaguchi, *J. Magn. Magn. Mater.* **140–144**, 905 (1995).
- <sup>44</sup>H. Wada, Y. Tanabe, K. Hagiwara, and M. Shiga, *J. Magn. Magn. Mater.* **218**, 203 (2000).
- <sup>45</sup>Guo Guanghua, M. V. Eremin, A. Kirste, N. P. Kolmakova, A. S. Lagutin, R. Z. Levitin, M. von Ortenberg, and A. A. Sidorenko, *Zh. Éksp. Teor. Fiz.* **120**, 910 (2001) [*JETP* **93**, 796 (2001)].
- <sup>46</sup>A. Kirste, R. Z. Levitin, M. von Ortenberg, V. V. Platonov, N. Puhmann, V. V. Snegirev, D. A. Filippov, and O. M. Tatsenko, *Fiz. Tverd. Tela (St. Petersburg)* **43**, 1661 (2001) [*Phys. Solid State* **43**, 1731 (2001)].
- <sup>47</sup>T. Fujiwara, H. Fujii, and T. Shigeoka, *Physica B* **281–282**, 161 (2000).
- <sup>48</sup>E. V. Sampathkumaran, S. Majumdar, R. Mallik, R. Vijayaraghavan, H. Wada, and M. Shiga, *J. Phys.: Condens. Matter* **12**, L399 (2000).

Translated by Steve Torstveit